

Experimental Investigation of Friction Stir Spot Welding of dissimilar AA5052-AA7075 Joints

Mian Zaeem Gulzar^{*1} and Salman Hussain²

¹Department of Industrial Engineering, University of Engineering and Technology, Taxila, 47080, Pakistan

²Department of Industrial Engineering, University of Engineering and Technology, Taxila, 47080, Pakistan

^{*}(zaeem.gulzar@students.uettaxila.edu.pk)

Abstract – Friction Stir Spot Welding (FSSW) has emerged as a transformative solid-state joining method with wide-ranging applications in industries such as automotive, aerospace, and electronics. This study delves into the difficulties of FSSW for dissimilar aluminum alloys, specifically AA5052 and AA7075, which exhibit distinct material characteristics. To address the challenges posed by these dissimilar materials, a systematic Taguchi experimental design was employed to analyze the influence of three key welding parameters: rotational speed (RS), plunge rate (PR), and plunge depth (PD) on the maximum failure load (MFL) of the welds. The findings revealed notable trends in MFL in response to variations in these parameters. Notably, MFL consistently increased with higher RS and PR levels, while the impact of PD exhibited a more complex relationship, initially decreasing MFL until a critical point and then gradually increasing it. Through Signal-to-Noise ratio analysis, optimal welding conditions were pinpointed, indicating that the highest MFL was achieved at RS level 3 (1400 RPM), PR level 3 (8 mm/min), and PD level 1 (2.1 mm). Furthermore, a robust regression equation was formulated to predict MFL accurately based on the selected parameters. With a goodness-of-fit of 95.42%, the model demonstrates its reliability for navigating the design space effectively. This study contributes valuable insights into optimizing FSSW for dissimilar materials, facilitating its adoption and advancement in diverse industrial applications.

Keywords – Friction Stir Spot Welding, Dissimilar Aluminum Alloys, Taguchi Analysis, Welding Parameters, Maximum Failure Load, Solid-State Joining

I. INTRODUCTION

Spot welded lap joints are widely used in automotive manufacturing for joining sheet metal components, ensuring structural integrity. In aerospace, they're employed in lightweight structures like aircraft panels. Household appliances such as refrigerators and washing machines rely on them for assembling metal parts. The electronics industry uses them for battery packs, ensuring strong electrical connections. Additionally, they're prevalent in HVAC applications for ductwork and ventilation systems. Their strength-to-weight ratio makes spot welded lap joints versatile and crucial in various industries. [1]

These joints can be achieved by riveting, resistance spot welding and friction stir spot

welding (FSSW) [2]. FSSW offers advantages over others and sought more attention in recent studies [3].

Friction stir spot welding (FSSW) is an innovative solid-state joining process used to join metals without traditional melting and solidification. It involves rotating a non-consumable tool with a specially designed geometry at high speeds and pressing it against two or more metal workpieces to be joined [4]. The frictional heat generated softens the metals without reaching their melting point, allowing the tool to plunge into the workpieces and form a joint. Once the tool is withdrawn, the softened metal cools and solidifies, creating a strong, defect-free weld. FSSW offers several advantages, including minimal distortion, reduced heat-affected zones, and enhanced mechanical

properties in the welded area. It is particularly well-suited for lightweight materials like aluminum and magnesium commonly used in aerospace and automotive industries [5]. FSSW is an eco-friendly, efficient, and precise welding technique, making it a valuable option for joining metals in various applications [6].

FSSW of dissimilar materials encounters a variety of challenges, including differing thermal properties, melting points, and hardness levels in the materials, which can make it challenging to find suitable welding parameters that accommodate both materials [7]. Undesirable intermetallic compounds can form at the weld interface, compromising joint integrity, mechanical properties, and corrosion resistance. Moreover, the varying thermal expansion coefficients of dissimilar materials can induce residual stresses, leading to deformation or cracking [8]. Achieving defect-free, reliable joints becomes intricate due to differing material behaviors [9]. The study focuses on providing suitable solution to the mentioned issues by utilizing taguchi analysis. [10]

II. MATERIALS AND METHOD

Dissimilar plates of aluminum AA5052 and AA7075 were selected for welding. The composition of the used material is presented in Table 1. The tool used in welding was crafted from tungsten carbide due to its high strength, hardness, and wear resistance at high temperatures.

Table 1. Material Composition

Material	Al	Fe	Si	Cu	Mn	Mg	Cr	Zn
AA5052	Bal.	0.40	0.25	0.1	0.1	2.4	0.28	0.1
AA7075	Bal.	0.24	0.08	1.5	0.06	2.4	0.2	5.8

The welding process was carried out on a milling machine. The motor of machine caused the tool to rotate at different RPM values. At desired RPM, rotating tool plunges into the plates and causes the deformation in the spot resulting in the achievement of joint. The welds were achieved at different parameter values of rotational speed (RS), plunge rate (PR) and plunge depth (PD). The parameters levels are presented in Table 2.

Table 2. Input Parameters and Levels

Input Parameters	Level 1	Level 2	Level 3
RS	1000	1200	1400
PR	2	5	8
PD	2.1	2.6	3.1

Utilizing the parameters levels an experimental design was formulated to investigate the maximum failure load (MFL) of the welds. A Taguchi experimental design with L9 array was used for analysis of output parameter namely maximum failure load (MFL). After measurement of MFL, results were recorded. The experimental design along with measurements of output parameter is presented in Table 3.

Table 3. Design of Experiment

Experiment #	RS (RPM)	PR (mm/min)	PD (mm)	MFL (N)
1	1000	2	2.1	1979
2	1000	5	2.6	2038
3	1000	8	3.1	2164
4	1200	2	2.6	2103
5	1200	5	3.1	2211
6	1200	8	2.1	2332
7	1400	2	3.1	2244
8	1400	5	2.1	2356
9	1400	8	2.6	2358

III. RESULTS AND DISCUSSION

A. Means Effect

The main effect plots for data mean used to reflect the trend of output parameters. The plot for MFL means is presented in Fig. 1. The plot depicts the increase in MFL with increase in RS throughout the range of 1000 to 1400 RPM. Additionally, it reflects the consistently increasing behavior of MFL with increasing PR. Finally, the varying behavior of MFL dependent on PD can be visualized. MFL initially decreased with increasing PD up to 2.6mm and then gradually increased.

The response table for data means reflecting the order of significance of input parameters is showcased in Table 4. It reflects that the most significant factor affecting MFL is RS followed by PR and PD respectively.

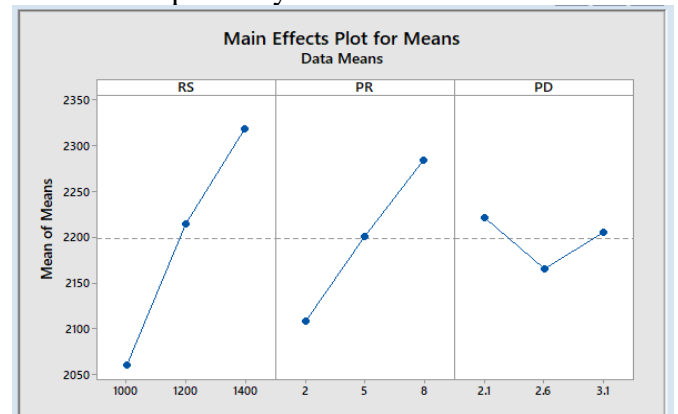


Fig. 1 Main effects plots for MFL means

Table 4. Response Table for Mean

Level	RS	PR	PD
1	2060	2109	2222
2	2215	2202	2166
3	2319	2285	2206
Delta	259	176	56
Rank	1	2	3

B. Signal to Noise Ratios

Signal to noise ratio determines those values of input parameters where output parameter is optimal. SN ratios for investigated output namely MFL are presented in Table 5. Mean effect plots depicted the trend of MFL with increase in parameters values.

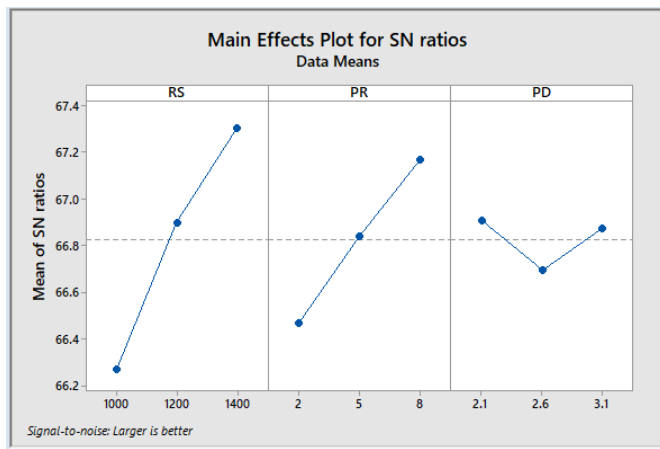


Fig. 2 Main effects plots for SN ratios

Table 5. SN Ratios

Level	RS	PR	PD
1	66.27	66.47	66.91
2	66.90	66.84	66.70
3	67.30	67.17	66.87
Delta	1.03	0.70	0.21
Rank	1	2	3

For MFL, larger the better characteristics of SN ratio were utilized as we wanted to maximize the MFL. From the plots of these SN values as in Fig. 2, it can be visualized that the optimal MFL was achieved at level 3 of RS (1400 RPM) as well as PR (8 mm/min) whereas for PD the optimal level was level 1 (2.1mm).

C. Regression Equation

To model the output parameter, a best fit line was developed which consisted of input parameters weighted by their contributed effect in the form of regression coefficients. The regression equation for prediction of MFL is presented below.

$$MFL = 1316 + 0.6475 RS + 29.33 PR - 16.0 PD$$

D. Model Summary

The adequacy of model was evaluated through few parameters which are presented Table 6.

Adeq. Precision measured the signal to noise ratio. A ratio greater than 4 was desirable. Observed ratio of 37.6205 indicated an adequate signal for MFL. The model is reliable to navigate the design space.

Furthermore, the R-sq value close to 100% was desired for adequacy. The achieved values of 95.42% reflect a good fit model.

R-sq (adj) and R-sq (pred) values were also found in close agreement with each other as their difference is less than 2% proving the adequacy of the model.

Table 6. Model Summary

Adeq. Precision	R-sq	R-sq (adj)	R-sq (pred)
37.6205	95.42%	92.67%	85.35%

E. ANOVA

ANOVA summarizes the model and factors significance. The ANOVA table for MFL is showcased in Table 7. From the table, it is evident that the model is significant which agrees with the model summary discussed already.

Furthermore, the significance of the factors can be extracted. The p-values for factor indicate that the significant input parameters are RS and PR in respective order whereas PD is comparatively insignificant.

Table 7. ANOVA for Output

Source	DF	Adj SS	Adj MS	F-Value	P-Value
Regression	3	147470	49157	34.73	0.001
RS	1	100622	100622	71.10	0.000
PR	1	46464	46464	32.83	0.002
PD	1	384	384	0.27	0.625
Error	5	7077	1415		
Total	8	154546			

IV. CONCLUSION

The FSSW joints between dissimilar AA5052-AA7075 were successfully created and analysed for MFL through Taguchi method. Mean effect plots depicted the trend of MFL with increase in parameters values. MFL consistently increased with increase in RS and PR whereas variation on PD initially caused it to decrease till 2.6mm and finally increase afterwards. SN ratios identified the optimal

parameters levels as RS3PR3PD1. Developed regression equation can be utilized to predict MFL with 95.42% goodness of fit.

REFERENCES

1. Shen, Z., Y. Ding, and A.P. Gerlich, *Advances in friction stir spot welding*. Critical Reviews in Solid State and Materials Sciences, 2020. **45**(6): p. 457-534.
2. Bagheri, B., et al., *Nanoparticles addition in AA2024 aluminum/pure copper plate: FSSW approach, microstructure evolution, texture study, and mechanical properties*. Jom, 2022. **74**(11): p. 4420-4433.
3. Abdollahzadeh, A., et al., *Advances in simulation and experimental study on intermetallic formation and thermomechanical evolution of Al–Cu composite with Zn interlayer: Effect of spot pass and shoulder diameter during the pinless friction stir spot welding process*. Proceedings of the Institution of Mechanical Engineers, Part L: Journal of Materials: Design and Applications, 2023. **237**(6): p. 1475-1494.
4. Siddharth, S. and T. Senthilkumar, *Optimization of friction stir spot welding process parameters of dissimilar Al 5083 and C 10100 joints using response surface methodology*. Russian journal of non-ferrous metals, 2016. **57**(5): p. 456-466.
5. Siddharth, S. and T. Senthilkumar, *Evaluation of Friction Stir Spot Welded Al 5083 Aluminium Alloy and C10100 Copper Dissimilar Joints*. Acta Microscopica, 2017. **26**(1): p. 1-10.
6. Siddharth, S. and T. Senthilkumar, *Development of friction stir spot welding windows for dissimilar Al5086/C10100 spot joints*. Materials Today: Proceedings, 2018. **5**(2): p. 6550-6559.
7. Wu, S., et al., *Conventional and swing friction stir spot welding of aluminum alloy to magnesium alloy*. The International Journal of Advanced Manufacturing Technology, 2021. **116**: p. 2401-2412.
8. Zhou, L., et al., *Microstructure evolution and mechanical properties of friction stir spot welded dissimilar aluminum-copper joint*. Journal of Alloys and Compounds, 2019. **775**: p. 372-382.
9. Zhou, L., et al., *Microstructure and mechanical properties of Al/steel dissimilar welds fabricated by friction surfacing assisted friction stir lap welding*. Journal of Materials Research and Technology, 2020. **9**(1): p. 212-221.
10. Chen, C., et al., *Investigation of a renovating process for failure clinched joint to join thin-walled structures*. Thin-Walled Structures, 2020. **151**: p. 106686.